CLEO: Closed-Loop kinematics Evolutionary Optimization of bipedal structures

Virgile Batto, Ludovic de Matteis, Thomas Flayols, Margot Vulliez, Nicolas Mansard

CLEO: Closed-Loop kinematics Evolutionary Optimization of bipedal structures

Virgile Batto[1,2,*], Ludovic De Matteïs[1,3],Thomas Flayols[1,4], Margot Vulliez[2], Nicolas Mansard[1,4]

***Abstract*— Progress in hardware design is crucial for achieving better artificial locomotion. There is a significant ongoing effort in the community to leverage dynamic capabilities of serial-parallel architectures in the design of humanoid legs. However, designing such systems involves addressing high-dimensional, complex, and multi-objective challenges, where conventional optimization approaches may encounter limitations or rely on additional know-how of the human designer.**

In this paper, we propose a general approach to assist the design of serial-parallel humanoid legs using an evolutionary optimization strategy. The optimization problem incorporates design constraints and locomotion-task requirements as objective functions. It uses parallelized trajectory evaluation for efficient exploration of the design space. The effectiveness of the design methodology is shown by optimizing a new leg architecture, that fully exploits the capabilities offered by kinematic closure. The optimized leg design meets practical constraints related to foot position, joint placement, and force transmission, ensuring stability and locomotion performance. We improve our design robustness by including several criteria that increase structural stiffness. The optimized leg exhibits desirable properties and matches the required simulation design constraints. Furthermore, we compare 3D-printed prototypes and experimentally validate the impact and choice of the design criteria.

I. INTRODUCTION

The development of novel, robust, and high-fidelity hardware is critical for more powerful control algorithms to be effective on real robots, especially in humanoid robotics. The integration of parallel mechanisms in modern humanoid robot legs is becoming increasingly common, particularly for the ankle joints [1], [2], [3]. Parallel mechanisms offer superior dynamic performance by reducing the leg effective inertia [4]. However, parallel leg architectures are more difficult to model and design due to their inherent trade-off between workspace and specific singularities [5], [6].

To address these challenges, codesign methods have emerged as promising approaches to the development of more sophisticated and efficient robotic legs. Codesign involves the simultaneous design of both the robot mechatronics and the control systems [7], to ensure optimal integration and performance. This approach has been successfully applied to the design of simple leg mechanisms [8], [9]. By designing the control algorithm alongside the mechanical structure and its actuation, the viability and performance of the robot can be significantly enhanced.

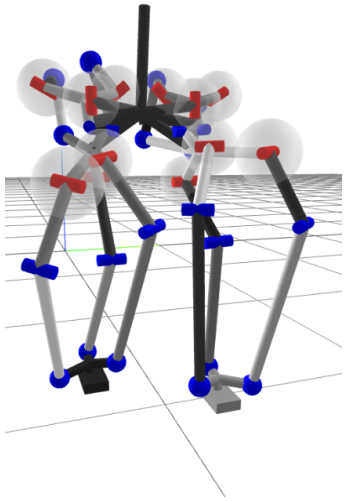

Fig. 1. A 3D view of the bipedal robot kinematics, featuring a novel serial-parallel architecture optimized through the CLEO algorithm.

A first challenge in codesign is to compute a dynamic movement for the targeted architecture [10]. Early works have demonstrated the feasibility for less complex robot codesign [11]. The emergence of efficient modeling libraries, such as Pinocchio [12], facilitates the incorporation of the contact constraints of parallel-kinematic chains, addressing the modeling difficulty [13]. While the computational complexity remains high, it can simulate any parallel architecture.

A second challenge is to properly define the design requirements by formulating an optimization problem. A bi-level optimization algorithm can be implemented for both the robot trajectory and the design parameters [14]. This method requires an efficient motion generation method that is yet to be developed for bipedal robots. We, therefore, propose to write a single-level formulation that can be solved as a gradient-free optimization. It decides the design variables without having to compute the sensitivity of the motion generator. Recent genetic algorithms and computational hardware advances make it possible to solve high-dimensional optimization problems, including those with complex Pareto fronts [15]. These methods have effectively solved various mechanical design optimizations [16]. Ranging from single-objective optimization of 6-DOF manipulators [17] to multi-objective optimization of parallel robots [18], they use performance objectives to determine the optimal design parameters.

*This work is suported by (1) Défi clé Robotique centrée sur l'humain (funded by Région Occitanie, France), (2) ROBOTEX 2.0 (ROBOTEX ANR-10-EQPX-44-01 and TIRREX-ANR-21-ESRE-0015), (3) Dynamograde (ANR-21-LCV3-0002) and (4) ASAP-HRC (ANR-21-CE10-0001)

[1] LAAS-CNRS, Université de Toulouse, CNRS, Toulouse, France
[2] Auctus, Inria, centre de l'Université de Bordeaux, Talence, France
[3] Inria, École normale Supérieure, PSL Research University, Paris, France
[4] Artificial and Natural Intelligence Toulouse Institute, France
* corresponding author: virgile.batto@laas.fr

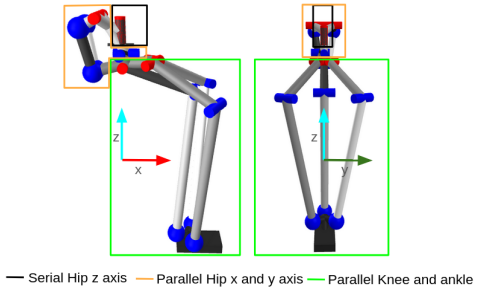

Fig. 2. Overview of the proposed architecture. The upper part allows for a range of rotational movements typically associated with the hip, yet with a serial-parallel structure. The lower part of the leg (3 DOF) is composed of 3 parallel branches actuating the knee and the roll and pitch of the ankle

However, applying such methods on complex humanoid leg structures, for which the locomotion tasks impose specific capabilities and strict constraints, has not been done yet.

This paper introduces CLEO, a gradient-free (evolutionary) optimizer for closed-loop kinematics biped codesign. The algorithm can optimize any generic architecture (serial or parallel) and decide the location of the motors and joints, as well as the actuation capability, with respect to several performance criteria and constraints. These requirements and design constraints must be appropriately chosen to meet the need of high-dynamic locomotion tasks [13]. While the shape of the different parts could also be considered a decision variable [19], topological optimization is too complex to be directly included within a codesign process. We decided to leave this topological work to the mechanical designer.

Section II proposes a novel bipedal architecture, mixing some features inspired by Tello [20] and Kangaroo [21]. If the proposed architecture is suitable for locomotion tasks, the behavior of such parallel mechanisms makes it quite counter-intuitive to decide the design parameter. They should be specifically optimized to obtain sufficient load capability on a large workspace. We then introduce CLEO, our main contribution, to optimize the design of the new architecture, in section III. Implementation details are given in section IV. We then describe the optimization results for the architecture in section V and compare the resulting flexibility on two physical prototypes of the lower part of the leg.

II. Leg Architecture

We propose a serial-parallel architecture that combines the advantages of the two parallel mechanisms: an upper parallel bar mechanism generates the roll-pitch motion of the hip, and a lower 3-RRS parallel structure provides the knee displacement and the roll-pitch motion of the ankle. The hip z axis is serially actuated since it is the less loaded articulation of a biped robot. The x and y axes are set in parallel to increase torque capability around the y-axis, one of the most torque-demanding directions. The last 3 degrees of freedom are set in parallel, within an architecture that aims at maximizing the z-axis force that the robot foot can produce, similarly to [22]. The kinematic diagram of this structure is presented in figure 2. While it offers structural benefits, its effective capability mostly relies on properly arranging the joint orientation and bar length. Given the complexity to optimize such a morphology, we develop an algorithm that can automatically select design parameters.

III. Optimization Algorithm

A. Algorithm overview

CLEO's primary objective is to optimize architectures of bipedal legs, by determining the parameters of the kinematic structure and the placement of the motors. These optimization parameters are denoted by the variable X. This includes variables that define joint positions, orientations, and motorization selection. By systematically adjusting these parameters, CLEO aims at identifying the optimal set of design parameters of the leg that maximizes performance criteria while satisfying all design constraints. We first present the optimization generic principles before providing details about the selected optimization criteria and constraints.

The optimization process employs the NSGA-III genetic algorithm [15], which is well-suited for handling high-dimensional, multi-objective optimization problems. This approach can simultaneously optimize multiple criteria, such as minimizing the leg inertia, maximizing its range of motion, and ensuring sufficient structural stiffness. By leveraging this genetic algorithm, CLEO efficiently explores the complex design space of bipedal leg architectures, and ultimately converges to a design configuration that provides superior performance. The optimized leg designs generated by CLEO are then validated through simulation and prototyping, ensuring their practical applicability in real-world scenarios.

B. Algorithm authority

The algorithm decides the motor models and placements, along with the linkage sizing and relative placement.

1) Motor Selection: The motor selection is a discrete variable denoted as X_m. Each value will refer to a motor from a range, noted MR of actuators, that will select :

- **Weight:** The mass of the motor, which impacts the overall weight distribution of the leg.
- **Inertia:** The moment of inertia of the motor, which affects the dynamic response of the leg.
- **Size:** The physical dimensions of the motor, ensuring it fits within the design constraints.
- **Reduction Ratio:** The gear reduction ratio, which will change the inertia of the motor axis.
- **Nominal Torque:** The continuous torque that the motor can deliver.
- **Peak Torque:** The maximum torque that the motor can deliver for a short period.

These parameters together form $X_m \in MR^6$, as the leg needs to have 6 actuated degrees of freedom.

2) Kinematic Structure: The kinematic structure is defined by a tree of joints with additional loop-closure constraints. Each joint is defined by its placement relative to its parent joint. The mass (m_{link}) of the linkage attached to a joint is proportional to its length (L_{link}), scaled by two factors respectively depending on the number of children ($N_{children}$)

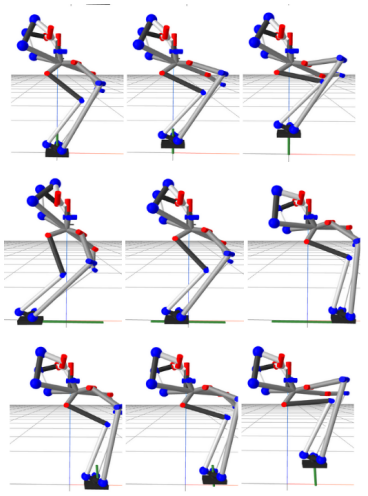

Fig. 3. We evaluate the design properties along 13 trajectories featuring pure translation or rotation, 3 of them being represented here (top row: vertical movement, mid row: forward movement, bottom row: offset vertical movement). Each of these trajectories is sampled with 60 points.

and reflecting the material. Here 0.3 is chosen to model the mass of an aluminum rod with a diameter of 10mm:

$$m = N_{children} \times L_{link} \times 0.3 \tag{1}$$

The inertia is computed from a homogeneous mass distribution, representing the segment as a tube. The motor masses are later added to obtain the final mass distribution.

Each degree of freedom (DoF) is either a revolute joint (conventionally around the z-axis) or a spherical joint. The algorithm determines the relative placement of each joint with respect to its parent: translation (3 parameters) and orientation (3 parameters using log representation). We also let the algorithm decide the orientation along the joint axes (either the z-axis for the revolute or the 3D orientation for the spherical joint) to get the mounting robot configuration. We sometimes want to inject additional designer knowledge by constraining some placement parameters. This should be considered at the constraints level. The motivation for introducing such knowledge is discussed in section III-G.9. We effectively implement it by clamping decision variables. Note that the decision variable defines movement around the base axis defined in the non-optimized architecture. Then, the joint orientation needs to be carefully chosen during the initial design of the architecture.

C. Decision variable

The kinematic parameters $X_k = [X_{k_1}, \ldots, Xk_{n_j}]$ modify the robot's kinematic structure, while X_m modifies its motorization. Together, they form the complete optimization parameter set $X = [X_m, X_k]$.

D. Workspace Evaluation

Ideally, the leg should be evaluated on a full locomotion trajectory. In practice, it is hardly possible as (i) the computational cost of generating such a movement remains too high to be integrated inside a genetic algorithm, and (ii) the robustness is insufficient to handle 100% of the candidate generated by the algorithm. We rather rely on a batch of 13 simpler trajectories, denoted $RT_i, i \in [1,13]$, that are representative of the difficulty of walking (see Fig. 3). We evaluated *a posteriori* that this simplification produces designs that can walk, as shown in the result section V.

E. Cost Function

We exploit our previous work [13] to define a multi-objective optimization problem that minimizes locomotion-based costs to get the Pareto front of optimal solutions.

1) Occupency volume: The leg's convex hull is the minimal convex shape that includes all its joints. Its volume v must be minimal to prevent the architectures from being unable to climb stairs or go through doors.

2) Foot inertia: To obtain a dynamic robot, the foot inertia is optimized. As the foot will mainly move in the sagittal plane, we minimize the foot inertia projected in this plane. Thus, with $\Lambda_A \in \mathbb{R}^6$ the foot effective inertia, the criteria to minimize can be written as:

$$g_2 = [\vec{z}, \vec{0}]\Lambda_A[\vec{z}, \vec{0}]^T \times [\vec{x}, \vec{0}]\Lambda_A[\vec{x}, \vec{0}]^T \tag{2}$$

3) Impact mitigation: As we want the leg to withstand impact, we also aim for a high-impact mitigation factor projected on the z-axis [23]. This criteria compares how the entire floating system reacts to external forces and how it reacts when the base is fixed. We compute the foot effective inertia when the base is non-fixed $\Lambda_{A_{free}}$ and when the leg is locked $\Lambda_{A_{lock}}$. We minimize the ratio projected on the z-axis to obtain a structure that will efficiently mitigate the impact.

$$g_3 = \frac{[\vec{z}, \vec{0}]\Lambda_{A_{free}}[\vec{z}, \vec{0}]^T}{[z, 0]\Lambda_{A_{lock}}[\vec{z}, \vec{0}]^T} \tag{3}$$

The second and third criteria are linked, as a low effective inertia will help mitigate the impact.

F. Multi-objective optimization

CLEO is developed as a tool to help robot designers to optimize their designs. A multi-objective problem is formulated rather than an arbitrary weighted sum. It provides a 3D Pareto front where designers can explore non-dominated solutions. The optimization problem is then written as:

$$\min_X \quad \begin{aligned} cost_1 &= \sum_{RT} \sum_{qi \in RT} v(X, qi) \\ cost_2 &= \sum_{RT} \sum_{qi \in RT} g_2(X, qi) \\ cost_3 &= \sum_{RT} \sum_{qi \in RT} g_3(X, qi) \end{aligned} \tag{4}$$

G. Constraints

A total of 9 constraints must be satisfied, primarily focusing on the foot position $P_f \in SE(3)$, with its translation denoted $P_{f_t} \in \mathbb{R}^3$ and the Jacobian matrix $J_a \in \mathbb{R}^{6\times6}$ that links the foot velocity to the actuator velocities.

1) Closed Loop Respect: In a closed-loop system, the loops within the architecture must remain unbroken. This requirement is enforced as a contact constraint condition, where the contact error $C_k \in \mathbb{R}^3$ must not exceed 5 cm:

$$\forall q \in RT_i, \forall q_i \in q, \forall k = 1 : n_k, \quad ||C_k(q_i;X)|| < \varepsilon_c \quad (5)$$

where C_k is the characteristic function of each of the n_k loop-closure constraints. The tolerance $\varepsilon = 5cm$ accommodates minor numerical integration errors along the trajectory. Here, we choose $5cm$ as the threshold value to trigger it only when the loop-closure constraints are no longer respected.

2) Compactness: We explicitly set boundaries to avoid generating leg architectures that cannot walk. The first constraint ensures that the foot is below any leg articulation.

$$\forall q \in RT_i, \forall q_i \in q, \forall j = 1 \dots n_j, \quad p_j(q_i,X).\vec{z} < P_{f_t}.\vec{z} + \varepsilon_f \quad (6)$$

where p_j is the position of the n_j joint and $\varepsilon_f = 0.02$ a safety margin. This enforces the foot to be $\varepsilon_f = 2cm$ lower than any other joint to account for joint occupancy. A similar boundary ensures the leg to remain oriented in the sagittal plane. Each articulation must be between $\varepsilon_l = 15cm$ left and $\varepsilon_r = 10cm$ right of the hip from the leg center:

$$\forall q \in RT_i, \forall q_i \in q, \forall j = 1 \dots n_j, \quad \varepsilon_r < p_j(q_i,X).\vec{y} < \varepsilon_l \quad (7)$$

Here, an asymmetry in the boundary gives more freedom while ensuring that the two legs can be placed 20 cm apart.

3) Static Capability: Each leg must sustain the robot's weight and produce sufficient force for walking to ensure stability. The absolute value of the Jacobian is used to accommodate worst-case force direction.

$$\forall q \in RT_i, \forall q_i \in q, \quad |J_a^T| F_{\text{walk}} < \tau_{mot} \quad (8)$$

The force set F_{walk} is defined to produce 110% of the robot weight $P = mg$ on the z-axis and 10% on the x and y-axes. The torque needed is chosen based on the torque generated on the foot of the robot Talos during stair climbing experiments, then scaled to the robot [24]:

$$F_{\text{walk}} = (0.1P \ , \ 0.1P \ , \ 1.1P \ , \ 0.02P \ , \ 0.02P \ , 0.01P) \quad (9)$$

4) Dynamic Capability: To enable running, the leg must simultaneously produce significant forces on the z and x-axes and torque around the y-axis of the foot. The leg can use the peak motor torque τ_{peak} :

$$\forall q \in RT_i, \forall q_i \in q, \quad |J_a^T F_{\text{run}}| < \tau_{peak} \quad (10)$$

The force set F_{run} is:

$$F_{\text{run}} = (0.5P \ , \ 0 \ , \ 2P \ , \ 0 \ \ , \ 0.01P \ , \ 0) \quad (11)$$

5) Kinematics Singularities: For every tested configuration, 1 rad/s on the actuators must generate at least 1 mm/s or 10^{-3} rad/s on the foot. The value has been chosen quantitatively to trigger kinematics singularities :

$$\forall q \in RT_i, \forall q_i \in q, \quad \frac{1}{\min\left(|J_a \cdot [1,1,1,1,1,1]^T|\right)} < 1000 \quad (12)$$

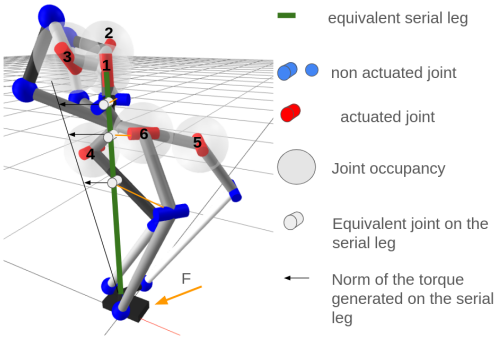

Fig. 4. Equivalent torque transmission on an ideal leg

6) Forces Singularities: A combination of 1 N and 1 Nm of force and torque in any direction on the foot must not generate more than 10 Nm of torque on the actuators. The value has been chosen quantitatively to trigger force singularities:

$$\forall q \in RT_i, \forall q_i \in q, \quad \max\left(|J_a^T \cdot [1,1,1,1,1,1]^T|\right) < 10 \quad (13)$$

The previous two criteria ensure non-proximity to singularity in the tested workspace.

7) Constraint Singularities: Constraint singularities [29] are inherent to parallel structures and lead to uncontrollable degrees of freedom. Being close to these singularities causes joint peak forces, leading to flexibility. To avoid this, we compare the force transmission on the joints between the parallel architecture and an ideal serial architecture. An ideal serial architecture is a simple bar touching the ground at the same point as the parallel one. A representation is shown in Fig 4. A force field is applied on the foot of both architectures. This force field will generate joint torques. We compare the torques applied to each joint of the parallel structure to the torque applied at the same height on the ideal leg. As we want the parallel structure to be stiffer, each joint on parallel mechanism should transmit less torque than the equivalent joint of the ideal leg. Here, we want the parallel leg to be at least 25% stiffer than the serial one. Thus, the norm of the torque generated on each joint needs to be 25% less.

$$\forall q \in RT_i, \forall j = 1 \dots n_j, \quad 1.25|\tau_j(q_0,X)| < |\tau_{serial}| \quad (14)$$

This calculation is computationally intensive, as the forces must be propagated inside a parallel structure. Thus, only the first point of each trajectory is evaluated. With 13 different trajectories, each with different starting points concentrated around the walking pattern, we ensure the stiffness of the leg during its lifecycle.

8) Joint Intersection: To obtain a buildable structure, joints or motors must not be too close. Each joint requires either a sphere of $r_j = 2cm$ radius, as it has been determined to be the minimal occupancy volume of the real mechanical joint, or a sphere of the motor radius $r_j = r_{mot}$ that doesn't

intersect with any other sphere of other joints.

$$\begin{aligned} \forall q \in RT_i, \forall q_i \in q, \forall j_1 = 1 \dots n_j, \forall j_2 = j_1 + 1 \dots n_j \\ ||p_{j_1}(q_i, X) - p_{j_2}(q_i, X)|| > r_{j_1} + r_{j_2} \end{aligned} \tag{15}$$

Figure 4 presents the occupancy of the actuated joint, with each joint sufficiently far from the others.

9) Manufacturability: The orientation of some joints should be limited to ensure the leg is easy to manufacture. Manufacturing a part supporting a motor or axis wholly misaligned from the parent axis is complicated. Thus, completely fixing the joint's orientation makes the part easy to make. Making the joint able to rotate only around the x or y axis (defined from his parent joint) doesn't add such complexity to the manufacturing part of the pieces, as intermediate pieces oriented with centering pins can be machined. As explained in Sec III-B.2, this constraint can be seen as a restriction of the parameter spaces. Then the joint can be let **free**, with **half free rotation**, or with **fixed orientation, free translation**. The designer chooses to ensure or not easier machining.

IV. Algorithm Implementation

The problem with hard constrain is finally written :

$$\begin{aligned} & & \text{cost}_1 &= \sum_{RT} \sum_{q_i \in RT} v(X, q_i) \\ & \min_X & \text{cost}_2 &= \sum_{RT} \sum_{q_i \in RT} g_2(X, q_i) \\ & & \text{cost}_3 &= \sum_{RT} \sum_{q_i \in RT} g_3(X, q_i) \\ & \text{subject to} & (4)\ to\ (14) &= 0 \end{aligned} \tag{16}$$

Given the complexity of the problem and the difficulty of producing the derivatives of the cost function and constraints, a gradient-free method is used. We employ the NSGA-III genetic algorithm [25], which supports high-dimensional cost functions and provides a good approximation of the Pareto front. For computational efficiency, the evaluation of the cost function is parallelized, with each trajectory $RT_i, i \in [1, 13]$ evaluated separately. This approach enables better workspace mapping without increasing computation time. The function is minimized when all constraints are equal to zero. It has been experimentally determined that the genetic algorithm converges better when the constraints are relaxed as penalties function and added as additional costs. The optimization problem is then implemented with 3 main costs and 4 additional penalties, each penalizing the violation of a constraint and which should be equal to zeros at convergence. The extra costs are :

$$\begin{aligned} \text{cost}_4 &= \sum_{RT} \sum_{qi \in RT} (c_{(4)} + c_{(5)}) \\ \text{cost}_5 &= \sum_{RT} \sum_{qi \in RT} (c_{(6)} + c_{(7)}) \\ \text{cost}_6 &= \sum_{RT} \sum_{qi \in RT} c_{(10)} \\ \text{cost}_7 &= \sum_{RT} \sum_{qi \in RT} c_{(11)} \end{aligned} \tag{17}$$

where $c_{(k)}$ is a linear penalty that penalizes the violation of the constraint (k) The generated Pareto front will be 3-dimensional when the constraints are respected.

V. Optimization result

A. Optimization parameter

The following degrees of freedom are allowed for the joints:

- All the spherical joints (7) are let **free**
- All the motor joints (6) are let **half free rotation**
- All the other joints (5) are let **fixed orientation, free translation.**

Each translational parameter can vary between $[-0.2m, 0.2m]$ (allowing each joint to move 20cm in any direction), and each rotational parameter can vary between $[-1.5\pi, 1.5\pi]$ (allowing free rotation). To represent the closed kinematic loop, we need to place a pair of frames to replace 5 spherical joints and impose 3D contact between them. Thus, we have 10 frames plus 2 joints left free. Furthermore, as stated in Sec III-B.2, the base orientation of each joint is left free, and the direction of the rotation for the **fixed orientation, free translation** joints (either x or y-axis) is left free thus, the dimensionality of the variable representing the kinematics is as follows: $dim(X_k) = 12 \times 6 + 6 \times 6 + 5 \times 4 = 128$ We have chosen the 10 most relevant motors for our application from the range offered by the manufacturer "My Actuator" [26]. Each motor will change the mass, occupancy, inertia, and armature of the joint with the value given by the manufacturers. There are six motors, so $dim(X_m) = 6$. A total of $dim(X) = 134$ parameters defines the leg structure. To avoid excessive iterations where the genetic algorithm searches for a feasible architecture, a feasible initial configuration vector X is provided to warm start CLEO, as in the base design, all axes are parallel or perpendicular, making the initial architecture singular. The genetic algorithm aims to improve this warm-start configuration vector, though it does not guarantee a global minimum will be reached. The optimization is performed on a population of 84 individuals, with the algorithm running for 800,000 iterations, corresponding to 40h of computation with 14 CPU cores of Intel Xeon E5-2695 v4 used.

B. Analysis of the Pareto front

On the Pareto front (Fig 5), all solutions are quite similar. To exhibit the similarity, we select two extreme cases, the one with minimal foot inertia (named *Lightfoot*) and oppositely the one with maximal foot inertia (named *Heavyfoot*).

C. Validation in simulation

CLEO analyzes the design capability with a simplified trajectory RT_i. Here, we cross-validate the relevance of the trajectory set by showing that it leads to a design capable of executing very dynamic movements such as walking fast, climbing stairs, or even jumping. Here, we analyze a fast-forward walk generated by trajectory optimization. A bipedal robot is generated by adding the symmetry of the leg (see Fig 1). We formulate a whole-body optimal control

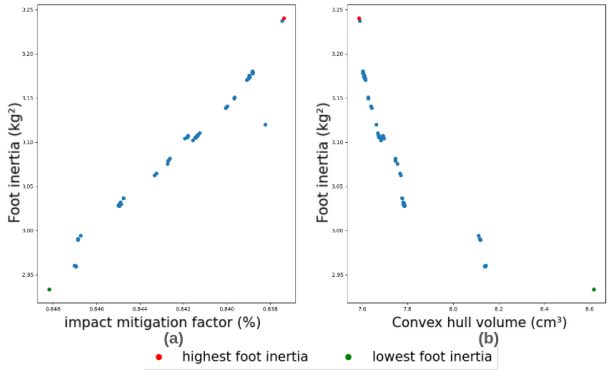

Fig. 5. Resulting Pareto front obtained using CLEO. **(a)** foot inertia against impact mitigation factor, and **(b)** foot inertia against Convex Hull Volume. We can see from (a) that the two criteria are quite equivalent

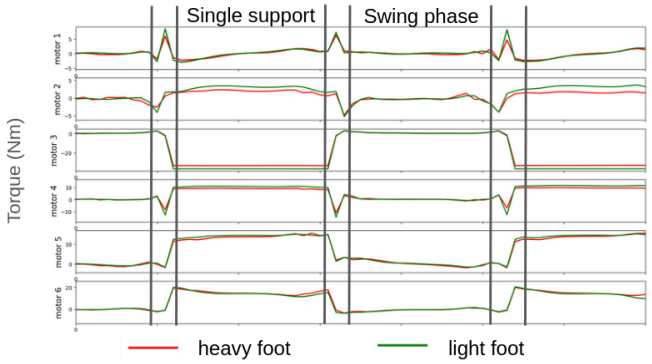

Fig. 6. Torque differences between 2 different legs on the Pareto front on a dynamics walking pattern

problem following the cost and constraints of [24] and using the complete dynamics model of the serial/parallel design using the differentiable dynamics described in [27],[28]. The walking speed is set to 1.5 m/s The resulting movement is presented in the companion video. It is smooth thanks to the singularity and generated forces cost in CLEO. The motor placement can be seen in Fig 4. In Fig 6, we display motor torques during a walking cycle for the two selected designs, *Light* and *Heavy* foot. Both designs have quite similar behavior, particularly minimal variation of torque demand during the swing phase, as the obtained leg inertia is very low. The torque needed during the support phase is higher for the *LightFoot* solution, which can be explained by a lower motor reduction chosen by CLEO to reduce the foot inertia. The algorithm has chosen a powerful motor for the exterior of the hip (joint 3), which can produce up to 30Nm, and we can see that it is needed to walk. The same OCP has been used to generate several gaits at different speeds and various configurations. The max torque does not show significant variation, particularly for higher dynamics. These movements are displayed in the companion video[1].

[1]https://peertube.laas.fr/w/kA9nDwcasftEk6mNntVEAd

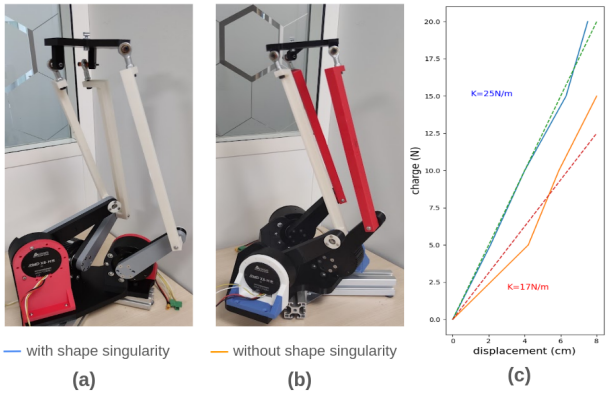

Fig. 7. The two prototypes compared in the study. (a) is the design resulting from complete optimization, (b) the result from partial optimization without constraint singularities cost. (c) The stiffness associated

D. Experimental validation of real hardware

The novelty of this design is the knee-ankle parallel mechanism, and no evidence of such a mechanism being used in humanoid legs has been found. While a design is not yet mature enough for a complete assembly, we seek to demonstrate its feasibility, particularly by investigating its stiffnesses (which is very difficult to do in simulation). Again, we selected two different designs for comparison. Both are chosen on the Pareto front to minimize foot inertia. The first results from a full optimization of CLEO (named *fully-optimized* design, seen in Fig 7).a), the second from a variation of CLEO where we remove the constraint related to constraint singularity $c_{(7)}$ (name *partially-optimized*, seen on Fig 7.a) In both cases, we only assembled the lower part of the leg with the 3-DoF corresponding to the knee and the ankle. We chose the solution maximizing the leg occupancy, as it is more straightforward to manufacture. Although they should have been assembled similarly, we printed the *fully-optimized* version with 10% infiltration and the *partially optimized* version with 40% infiltration. This error will be corrected later but will not prevent a relevant experimental analysis. The fully optimized design exhibits a much stiffer behavior, as shown in Fig 7.c. On the *partially optimized* design, 5N force on foot generates significant displacement (despite stiffer plastic pieces). With the $c_{(7)}$ active, the leg is much stiffer. This proves that the constraint singularities criterion enabled the generation of a stiffer architecture and that the genetic algorithm provide manufacturable results.

VI. Conclusion

In this work, we presented an effective approach to optimize serial-parallel leg architectures of a humanoid robot. It uses a gradient-free optimization method to manage the high-dimensional design space. By converting constraints into objective functions and leveraging parallelized trajectory evaluations, we identified optimal configurations that ensure practical viability. Simulation and hardware validations confirmed that the optimized leg meets all constraints, demonstrating robust performance under realistic conditions.

Key results highlighted the preference for designs achieving a balance between volume and inertia. The integration of a whole-body control algorithm confirmed the leg's ability to support the robot's weight and execute dynamic walking motions. Additionally, incorporating singularity constraints significantly improved the structural stiffness of the leg.

This study underscores the importance of considering both kinematic and inertial factors in leg design and shows the potential of genetic algorithms for complex robotic design tasks. Future work will aim to enhance the optimization process by including advanced dynamic models and expanding the approach to other robotic subsystems.

REFERENCES

[1] Agility Robotics. (2019) Digit advanced mobility for the human world. [Online]. Available: https://www.agilityrobotics.com/robotsdigit

[2] Unitree. (2024) Humanoid agent AI avatar https://www.unitree.com/g1/

[3] Boston Dynamics (2024), Atlas® and beyond: the world's most dynamic robots, https://bostondynamics.com/atlas/

[4] Jin, Xiaodong, Yuefa Fang, Haibo Qu, et Sheng Guo. "A Class of Novel 4-DOF and 5-DOF Generalized Parallel Mechanisms with High Performance". Mechanism and Machine Theory 120 (february 2018): 57-72. https://doi.org/10.1016/j.mechmachtheory.2017.09.015.

[5] Merlet, Jean-Pierre. Parallel robots. Vol. 128. Springer Science & Business Media, 2006.

[6] Park, F. C.,and Jin Wook Kim. "Manipulability of Closed Kinematic Chains". Journal of Mechanical Design 120, (1 december 1998): 542-48. https://doi.org/10.1115/1.2829312.

[7] Censi, Andrea. "A Class of Co-Design Problems With Cyclic Constraints and Their Solution". IEEE Robotics and Automation Letters 2, (january 2017): 96-103. https://doi.org/10.1109/LRA.2016.2535127.

[8] Fadini, G., Flayols, T., Del Prete, A., Mansard, N., & Souères, P. (2021, May). Computational design of energy-efficient legged robots: Optimizing for size and actuators. In IEEE International Conference on Robotics and Automation (ICRA)

[9] Gkikakis, Antonios Emmanouil. Mechanism and behaviour Co-optimisation of high performance mobile robots. 2021. PhD thesis. University of Genoa.

[10] Wensing, Patrick M., Posa, Michael, Hu, Yue, et al. Optimization-based control for dynamic legged robots. IEEE Transactions on Robotics, 2023.

[11] Langard, M., Ph. Lucidarme, N. Delanoue, R. Guyonneau, F. Mercier, C. Chevallereau, Ph. Wenger, et Y. Aoustin. "Design and Optimization of a Planar Biped Leg Based on Direct Drive Linear Actuators". Mathematical Problems in Engineering 2022 : 1-15. https://doi.org/10.1155/2022/6455182.

[12] Carpentier, Justin, Budhiraja, Rohan, et Mansard, Nicolas. Proximal and sparse resolution of constrained dynamic equations. In: Robotics: Science and Systems 2021.

[13] Batto, Virgile, Flayols, Thomas, Mansard, Nicolas, et al. Comparative metrics of advanced serial/parallel biped design and characterization of the main contemporary architectures. In : IEEE-RAS International Conference on Humanoid Robots (Humanoids) 2023

[14] Fadini, G. (2023). A versatile co-design framework for simultaneous optimization of robots' hardware and control (PhD thesis, Université Paul Sabatier-Toulouse III).

[15] Seada, H., & Deb, K. (2015). U-NSGA-III: a unified evolutionary optimization procedure for single, multiple, and many objectives: proof-of-principle results. In International conference on evolutionary multi-criterion optimization (pp. 34-49). Cham: Springer International Publishing.

[16] Qu, Zhanghao, et al. "Optimal design of agricultural mobile robot suspension system based on NSGA-III and TOPSIS." Agriculture 13.1 (2023): 207.

[17] Bjørlykhaug, Emil, and Olav Egeland. "Mechanical design optimization of a 6DOF serial manipulator using genetic algorithm." IEEE Access 6 (2018): 59087-59095.

[18] Stan, Sergiu-Dan, Radu Balan, and Vistrian Maties. "Multi-objective design optimization of mini parallel robots using genetic algorithms." 2007 IEEE International Symposium on Industrial Electronics. IEEE, 2007.

[19] Sigmund, Ole et Maute, Kurt. Topology optimization approaches: A comparative review. Structural and multidisciplinary optimization, 2013, vol. 48, no 6, p. 1031-1055.

[20] Sim, Youngwoo, and Joao Ramos. "Tello leg: The study of design principles and metrics for dynamic humanoid robots." IEEE RAL 7.4 (2022): 9318-9325.

[21] Roig, Adria, et al. "On the hardware design and control architecture of the humanoid robot kangaroo." 6th workshop on legged robots during the international conference on robotics and automation (ICRA 2022). 2022.

[22] Raw, L., Fisher, C., & Patel, A. . Effects of limb morphology on transient locomotion in quadruped robots. In 2019 IEEE/RSJ International Conference on Intelligent Robots and Systems (IROS) (pp. 3349-3356). IEEE.

[23] Wensing, Patrick M., et al. "Proprioceptive actuator design in the mit cheetah: Impact mitigation and high-bandwidth physical interaction for dynamic legged robots." Ieee transactions on robotics 33.3 (2017): 509-522.

[24] Dantec, E., Naveau, M., Fernbach, P., Villa, N., Saurel, G., Stasse, O., ... & Mansard, N. (2022, November). Whole-body model predictive control for biped locomotion on a torque-controlled humanoid robot. In 2022 IEEE-RAS 21st International Conference on Humanoid Robots (Humanoids) (pp. 638-644). IEEE.

[25] Liu, Q., Liu, X., Wu, J., & Li, Y. (2019). An improved NSGA-III algorithm using genetic K-means clustering algorithm. Ieee Access, 7, 185239-185249.

[26] https://www.myactuator.com/rmd-xplanetary-motor-1

[27] Budhiraja, Rohan, et al. "Differential dynamic programming for multi-phase rigid contact dynamics." 2018 IEEE-RAS 18th International Conference on Humanoid Robots (Humanoids). IEEE, 2018.

[28] Nganga, J. N., & Wensing, P. M. (2021). Accelerating second-order differential dynamic programming for rigid-body systems. IEEE RAL

[29] Zlatanov, D., Bonev, I. A., & Gosselin, C. M. Constraint singularities of parallel mechanisms. In Proceedings 2002 IEEE international conference on robotics and automation (Cat. No. 02CH37292) (Vol. 1, pp. 496-502). IEEE.